Displacement-Based Seismic Design for Reinforced Masonry Shear-Wall Structures, Part 2: Validation with Shake-Table Tests

Farhad Ahmadi,[a] Marios Mavros,[b] Richard E. Klingner,[c] Benson Shing,[d] and David McLean[e]

This paper provides a comprehensive validation of a displacement-based seismic design procedure proposed in a companion paper for reinforced masonry shear-wall structures. For this purpose, a full-scale, two-story reinforced masonry specimen was tested on a shake table to examine the global and local behaviors of a low-rise reinforced masonry building designed by the proposed displacement-based procedure, and to validate the analytical tool used in the design process. This specimen successfully resisted repeated ground motions with intensities up to the maximum considered earthquake (MCE). Its performance on the shake-table demonstrates that a reinforced masonry structure designed, detailed, and constructed according to the proposed displacement-based design procedure can resist MCE earthquakes without collapse even though it may suffer severe damage. In critical regions of this specimen, elements detailed in accordance with displacement-based requirements showed more inelastic deformation capacity than the deformation limits imposed by the displacement-based design provisions proposed here. The proposed procedure produces structures that behave according to design expectations, even though severely damaged. [DOI: 10.1193/120212EQS345M]

INTRODUCTION

A displacement-based design procedure and guidelines for reinforced masonry shear-wall structures are presented in a companion paper by Ahmadi et al. (2015, this issue). That paper includes a trial application to a full-scale, two-story, wall structure belonging to seismic design category (SDC) D according to ASCE 7-10 (2010). The purpose of that design was to demonstrate the application of displacement-based design to a low-rise building whose behavior was controlled by shear-critical wall segments. Conventional

[a] Postdoctoral Research Associate, Dept. of Civil Engineering, The University of Texas at Austin, 1 University Station C1700, Austin, TX 78712
[b] Graduate Research Assistant, Dept. of Structural Engineering, University of California, San Diego, 9500 Gilman Dr., La Jolla, CA 92093
[c] L. P. Gilvin Professor in Civil Engineering, The University of Texas at Austin, 1 University Station C1700, Austin, TX 78712
[d] Professor, Dept. of Structural Engineering, University of California, San Diego, 9500 Gilman Dr., La Jolla, CA 92093
[e] Professor, Dept. Civil Engineering, Washington State University, 405 Spokane Street, Sloan 101, Pullman, WA 99164

Earthquake Spectra, Volume 31, No. 2, pages 999–1019, May 2015; © 2015, Earthquake Engineering Research Institute

force-based approaches are not rational for such a structure, because they include the inherent assumption of a ductility capacity that can be far beyond what could be delivered with the structural configuration and associated inelastic mechanism. In this paper, the trial design is evaluated with shake-table testing and nonlinear time-history analyses to assess the validity of the design procedure and guidelines presented in the companion paper. The evaluation is based on several criteria. The first is to compare the actual inelastic mechanism and local deformations exhibited by the structure under the design earthquake (DE) and maximum considered earthquake (MCE) to those expected in the design process. The second is to examine whether the performance of the structure under DE- and MCE-level shaking is consistent with the performance objectives (story-drift limits and collapse prevention) intended in the design.

The shake-table tests presented here provide valuable insight into the system-level performance of modern low-rise reinforced masonry wall structures, and also provide the data necessary to validate the analytical tools that are central to displacement-based design. Only limited shake-table testing has been conducted on reinforced masonry structures designed and built according to modern U.S. practice. Within the research program carried out by the Technical Coordinating Committee for Masonry Research (TCCMAR), Seible et al. (1994a, 1994b) tested a full-scale, five-story reinforced masonry structure, to evaluate design recommendations and details developed for strength design, using pseudo-dynamic testing to simulate its earthquake response. Gülkan et al. (1990a and 1990b) tested a series of single-story, one-third-scale, masonry structures on a shake table to verify prescriptive reinforcing details for reinforced masonry shear walls in moderate seismic zones. Abrams and Paulson (1991) tested two three-story, quarter-scale, reinforced masonry structures to evaluate the accuracy of small-scale testing for these types of structures. Cohen (2004a and 2004b) tested two low-rise, half-scale, reinforced masonry buildings with flexible roof diaphragms on a shake table, and compared test results with results of quasi-static testing and analytical predictions. Jo (2010) tested full-scale concrete masonry wall segments with clay masonry veneer quasi-statically with out-of-plane and in-plane loads. Identical wall segments also were tested on a shake table, as was a full-scale, one-story structure (Klingner et al. 2010). Stavridis et al. (2012b) tested a full-scale, three-story, reinforced masonry structure designed according to current force-based design provisions (ASCE 2010). However, no shake-table validation tests have been conducted on reinforced masonry structures designed with displacement-based procedures.

DESIGN OF TWO-STORY REINFORCED MASONRY STRUCTURE

The displacement-based design of the full-scale, two-story, reinforced masonry structure tested on the shake table is described in the companion paper by Ahmadi et al. (2015). The test structure represented a portion of a typical two-story apartment or office building with a perforated reinforced masonry wall system. A view of the structure on the shake table is shown in Figure 1. As shown in Figure 2, the structure was rectangular in plan, with out-to-out dimensions of 22.67 ft in the direction of shaking and 20.67 ft perpendicular to the direction of shaking. The wall in the direction of shaking consisted of two T-wall segments (Walls W-1 and W-3) and one lineal wall segment (Wall W-2). The walls perpendicular to the direction of shaking were two lineal half-walls. Figure 2 also shows an elevation view of the structure in the direction of shaking, indicating the locations and

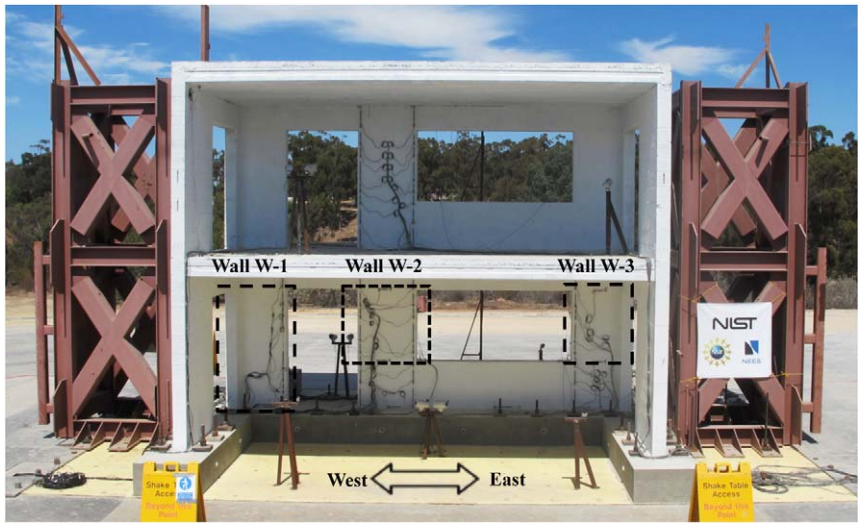

Figure 1. Full-scale two-story structure as constructed on the UCSD shake table.

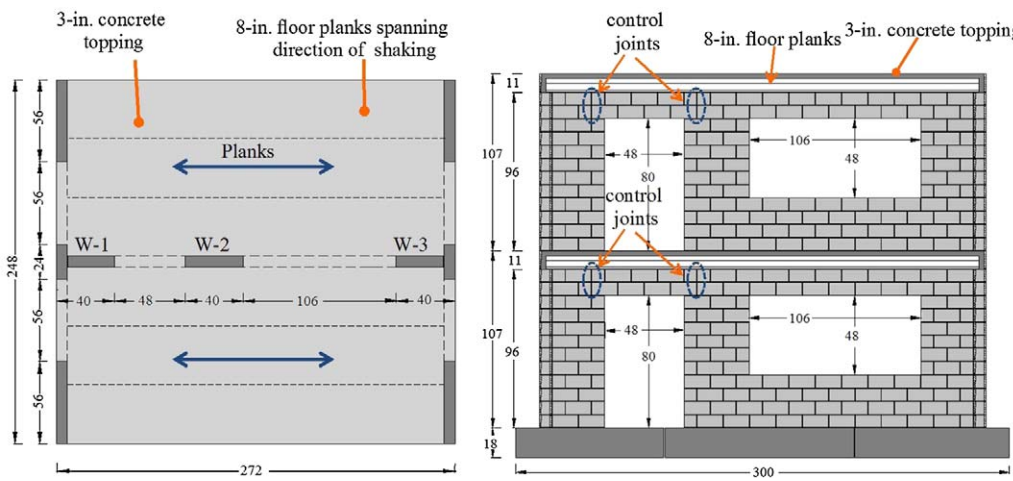

Figure 2. Plan view of typical floor and elevation view of the full-scale two-story specimen in direction of shaking (dimensions in inches).

configuration of the openings. As shown in Figure 2, control joints were introduced on each side of the lintel beams above door openings. The specimen used nominal 8-in. lightweight concrete masonry units (CMU) conforming to ASTM C90 (2011); ASTM C270 (2012) Type S cement-lime mortar by proportion; and ASTM C476 (2010) coarse grout by proportion. The walls were fully grouted. The floor and roof diaphragms were composed of prestressed 8-in.-thick hollow-core concrete planks, spanning parallel to the direction of

shaking, bearing on out-of-plane lineal walls and on flanges of T-walls, with 3-in.-thick reinforced concrete topping.

The specimen was designed using the displacement-based design procedure and guidelines proposed in this research (Ahmadi et al. 2015). In that procedure, an initial design was developed based on the draft limit-design requirements of the 2013 MSJC *Code*, including reinforcement requirements for shear- and flexure-critical reinforced masonry shear wall elements. Wall W-1 was considered flexure-critical and Walls W-2 and W-3 were shear-critical. A pushover analysis was then conducted to calculate the base shear and local deformations developed at the target displacement limits for the DE and MCE levels. The calculated base shear values were checked against the required base shear capacities calculated in the displacement-based design procedure using the displacement response spectra determined for the respective hazard levels and the expected equivalent viscous damping ratios. In addition, the local deformation demands and wall behavior were checked to ensure that they complied with the expected deformation limits and performance. For this case, the initial design turned out to be satisfactory. The reinforcing details for the structure are shown in Figure 3. The

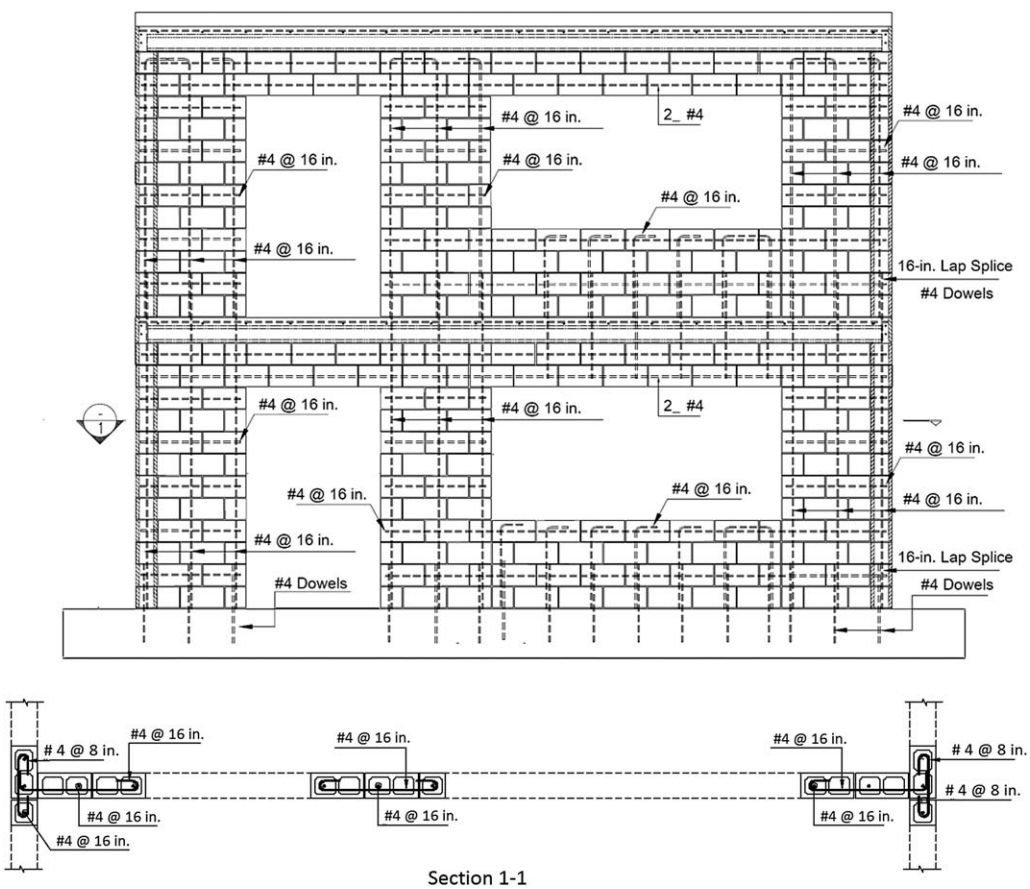

Figure 3. Reinforcing details of two-story masonry structure.

design did not meet prescriptive requirements for reinforcement in the 2011 MSJC *Code* for "special" reinforced masonry shear walls, as it would have been required for SDC D. As shown in Figure 3, Wall W-2 and the webs of Walls W-1 and W-3 had No. 4 bars at 16 in. for flexural reinforcement. Transverse reinforcement consisting of No. 4 bars at 16 in. for all walls. The prescriptive requirements of the 2011 MSJC *Code* would require a maximum bar spacing of no more than 13 in. for both longitudinal and transverse reinforcement.

PREDICTED RESPONSE OF TWO-STORY STRUCTURE

Using nonlinear time history analysis, the response of the trial design of the two-story structure to different ground motions was predicted and compared with performance objectives (story drifts and local deformation ratio limits) proposed for displacement-based design in the companion paper (Ahmadi et al. 2015). The analytical model was developed using General Wall Elements, which are macro elements implemented in PERFORM-3D (CSI 2007). Details and calibration of the structural model are given in Ahmadi et al. (2015). The structural model was subjected to scaled ground motions from the 1979 Imperial Valley earthquake (El Centro array #5, 140 degrees) and 1999 Chi Chi earthquake. The motions were scaled to DE and MCE levels based on the spectral acceleration corresponding to the initial elastic period of the structure (0.09 s). For DE, the 1979 El Centro and 1999 Chi Chi records were scaled to 89% and 68%, respectively. For MCE, they were scaled to 135% and 102%, respectively. The structure had different gravitational mass and seismic mass because of the different tributary areas assumed for the two types of mass. The seismic mass was 1.7 times the gravity mass. However, in the analysis, only the gravitational mass was specified and the seismic mass was accounted for by scaling the ground motion records in time and amplitude, as explained in the next section on shake-table testing.

Results of the time-history analyses are summarized in Table 1, including the maximum predicted deformation demands in ground-level wall segments W-1, W-2, and W-3; maximum base shear; and maximum story drifts. The maximum deformation demands are the maximum relative lateral displacement between ends of each wall segment divided by the height of that segment, and are expressed in percent. The total lateral displacement of each wall segment includes flexural deformation and shear deformation. Results show that Walls W-2 and W-3 were critical, with the highest predicted local deformation ratios and the lowest

Table 1. Results of time-history analyses for trial design of two-story specimen

Ground motion		Story drift in ground level, %		Base shear, kips	Maximum local deformation ratio, %		
		West direction	East direction		W-1	W-2	W-3
EC-DE	89% El Centro	0.14	0.26	163	0.31	0.52	0.52
CHI-DE	68% Chi Chi	0.43	0.24	158	0.26	0.52	0.44
EC-MCE	135% El Centro	0.24	0.44	195	0.52	0.92	0.96
CHI-MCE	102% Chi Chi	0.52	0.36	203	0.57	1.13	0.98

deformation capacities, because these segments were shear-controlled. Wall W-1 was a flexure-controlled component, but had smaller deformation demands. Figure 4 shows the maximum predicted local deformation ratios in ground-level wall segments W-1, W-2, and W-3 under the MCE-level ground motions. Figure 5 shows time histories of story drift ratios under MCE-level ground motions. According to the local deformation ratio limits proposed by Ahmadi et al. (2015) for displacement-based design of reinforced masonry shear walls, Wall W-1, which was flexure-controlled, had deformation limits of 0.8% and 1.5%

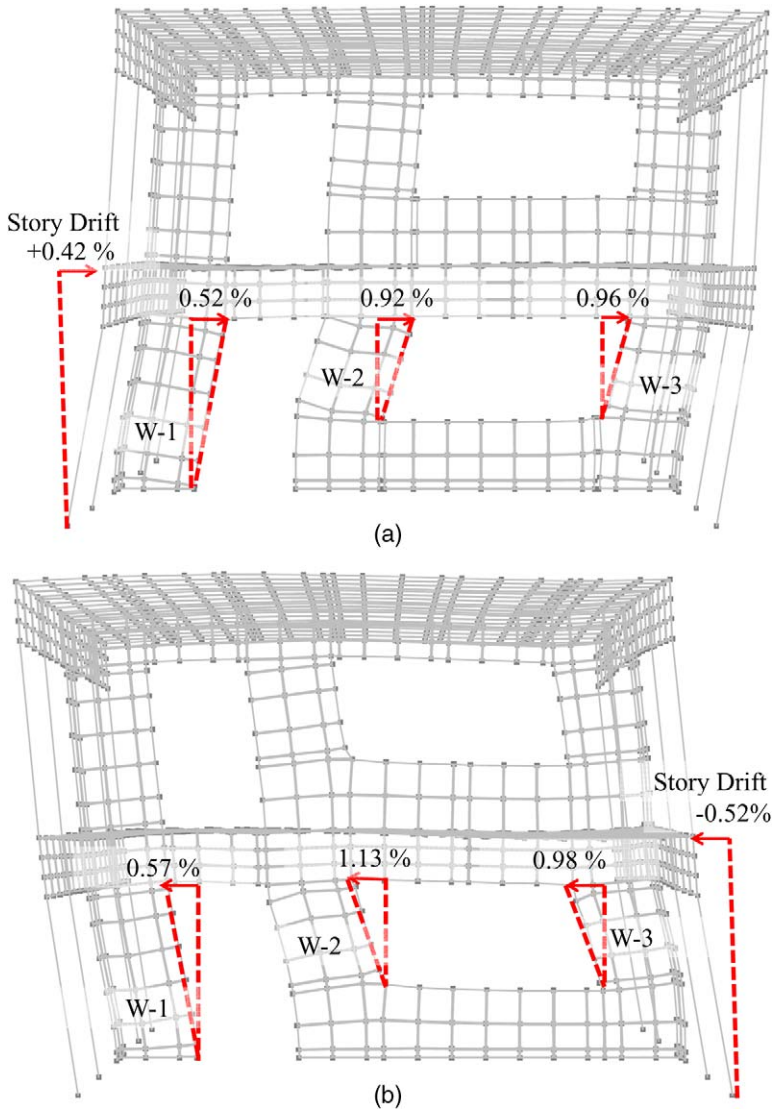

Figure 4. Maximum predicted local deformation ratios for trial design under MCE-level ground motions: (a) 135% El Centro ground motion; (b) 102% Chi Chi ground motion.

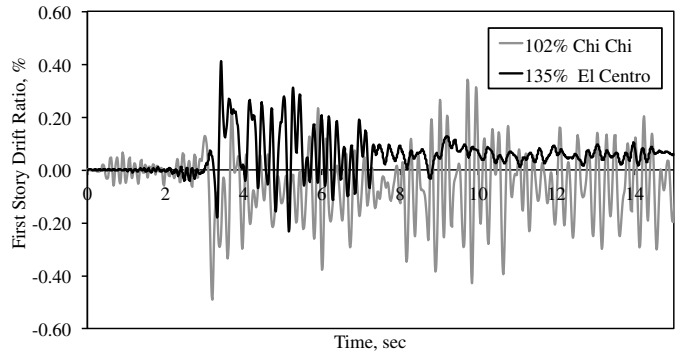

Figure 5. Time histories of story drift ratios for trial design under MCE-level ground motions.

for DE and MCE, respectively, while Walls W-2 and W-3, which were shear-controlled, had limits of 0.5% and 1.0%. By comparing these limits to the analysis results, it can be observed that they were only slightly violated for the shear-controlled walls. As explained in Ahmadi et al. (2015), the story-drift limits used for this design were 0.3% for DE and 0.6% for MCE. This was only slightly violated for the case of the El Centro design level motion. Hence, the design can be considered satisfactory.

SHAKE-TABLE TESTS OF TWO-STORY TRIAL DESIGN

The trial design of the two-story reinforced masonry structure was tested on the Large High-Performance Outdoor Shake Table (LHPOST) at the Englekirk Structural Engineering Center of the University of California, San Diego (UCSD). The reinforced concrete foundation of the test structure was tied onto the table by post-tensioned threaded steel rods. The table has plan dimensions of 7.60 m × 12.20 m (25 ft × 40 ft) and has a maximum payload capacity of 20 MN (450 kips). The two hydraulic actuators controlling the table motion have a stroke of ± 0.75 m (29.5 in.), and are capable of driving the table to a maximum velocity of 1.80 m/s (70 in./s). It currently operates in a single-degree-of-freedom configuration, with motion in the east-west direction only. Technical characteristics of the LHPOST are described by Ozcelik et al. (2008).

INPUT GROUND MOTIONS

The two-story test structure was designed for a seismic mass that was 1.70 times what would have been implied by the actual footprint of the structure. This increase in the tributary seismic mass was to ensure that the structure could be designed to barely meet the demand calculated with the displacement-based procedure without redundant capacity. This additional mass was not physically presented in the test structure, but rather was accounted for in the tests by scaling up the input ground accelerations by a factor of 1.7 and compressing the time scale by a factor of $1/\sqrt{1.70}$ to satisfy the dynamic similitude requirements. The aforementioned scaling introduced the same effect as added mass as explained in Harris and Sabnis (1999), Stavridis et al. (2012a), and Ahmadi (2012).

For the shake-table tests, an El Centro record (array #5, 140 degrees) from the 1979 Imperial Valley earthquake was selected because the shape of its acceleration spectrum matches the design spectrum (ASCE 2010) relatively well for the period range of interest (0 s to 0.5 s). The record was scaled in time to satisfy the similitude requirements, as mentioned above, and the test structure was subjected to six earthquake motion time histories of gradually increasing intensities, with accelerations scaled to 30%, 43%, 86%, 108%, 145%, and 160% of the El Centro record, respectively, on top of the scale factor of 1.70 required to account for the increased seismic mass. Before each earthquake ground motion history, the structure was tested using 3 minutes of low-amplitude white-noise (WN) excitation. These tests were conducted to identify the dynamic properties of the structure before and after each seismic history, so that the change of natural periods and mode shapes due to the induced damage could be observed. The white-noise record consisted of 0.5–25-Hz band-clipped acceleration processes with root mean square (RMS) amplitude of 0.03 g. The amplitude was low enough not to induce additional damage to the structure. The natural periods of the structure were identified from the transfer functions calculated from the acceleration time histories measured at the base and the roof of the structure.

To correct for the influence of the table-actuator dynamics, each input record was modified with the transfer function of the empty table identified for each amplitude level prior to the tests. However, that correction did not account for the dynamic properties of the test structure, which changed as damage evolved in the tests. As a result, the output motions from the table were not exactly identical to the input. A sample table output motion measured at foundation level for the 86% El Centro record is shown in Figure 6. The elastic 5% damped acceleration response spectra for the 108% and 160% El Centro motions measured from the table are also shown in Figure 7, together with the fundamental periods of the structure identified by white-noise excitation prior to each motion, as well as the DE and MCE response spectra used for the design. Based on the fundamental period identified prior to each motion, it can be observed that 108% El Centro corresponds to DE, while 160% El Centro corresponds to MCE. The initial fundamental period of the structure was 0.07 s; at the beginning of 106% El Centro, which was the very last shaking, it was 0.21 s; and at the end of testing, it

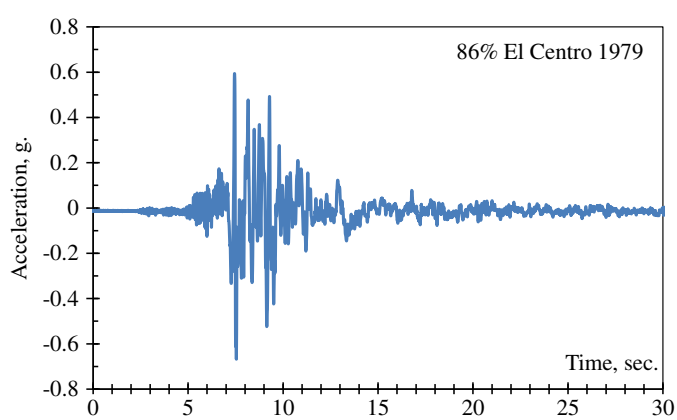

Figure 6. Sample table motion (86% El Centro 1979).

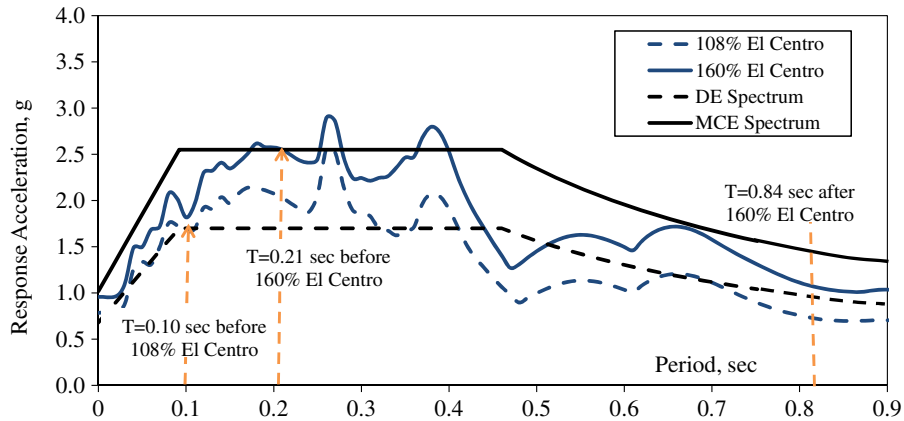

Figure 7. Response spectra of table motions corresponding to 108% and 160% El Centro.

was about 0.84 s. The acceleration response spectrum of 160% El Centro, as reproduced on the shake table, had two pronounced peaks at 0.27 s and 0.38 s, which were in the period range of the test structure during that run (0.21 s to 0.84 s).

OVERALL OBSERVATIONS

In Table 2, the key behaviors of the two-story structure at different ground motion intensities are summarized, along with the level of excitation, as compared to DE and MCE, and Peak Ground Acceleration (PGA). These PGAs were measured from the table output motions. The PGA for 160% El Centro was less than that for 145% El Centro because of interaction between the table and structure, and because of the progressive damage suffered by the structure during the two motions, which changed its dynamic properties.

Initial response of the two-story specimen was marked by vertical and horizontal cracks at the dog-leg control joints (shown in Figure 2) at both ends of the lintel connecting Walls W-1 and W-2. At DE-level ground motion (108% El Centro 1970), cracks formed at the edges of the ground-floor window opening (Figure 8). Although the longitudinal reinforcement passing through the lintel had been de-bonded on one side of each control joint, the strong connection between the precast planks and the wall segments caused the lintels to move with the planks rather than the walls, and caused some lintel cracking. In addition, flexural cracks formed at the base of Wall W-1, and a diagonal crack formed below Wall W-3.

As shown in Figure 9, continued shaking with 160% El Centro (MCE) caused distributed flexural and shear cracks in Wall W-1 (Figure 10a); significant sliding at the top of Wall W-2 at the beginning of shaking; followed by extensive diagonal cracks and shear failure of Wall W-2 (Figure 10b); the widening of shear cracks in Wall W-3 (Figure 10c); the crushing of the diagonal struts and face-shell spalling in Walls W-2 and W-3; and out-of-plane flexural cracking at the bases and tops of the out-of plane walls. In addition, this ground motion

Table 2. Summary of test history and specimen response

Ground motion	Level of excitation	Measured PGA from table	Observations
30% El Centro		0.27 g	No visible damage was observed. Structural period T before and after test was about 0.07 s.
43% El Centro	0.50 DE	0.39 g	Hairline cracking was observed at the bases of the W-1 wall segment and out-of-plane walls; max. 1st story drift = 0.03%.
86% El Centro		0.66 g	Further hairline cracking was observed at the bases of the W-1 wall segment and out-of-plane walls, indicating flexural cracking; flexural cracks developed at ends of lintel beam near control joints and the window opening corners at the first floor; a diagonal crack observed below W-3 wall segment; max. 1st story drift = 0.12%; structural period after test was about 0.09 s.
108% El Centro	DE	0.75 g	More cracking was observed at the bases of the W-1 wall segment and out-of-plane walls; more cracks developed at ends of lintel beam near control joints and the window opening corners at the first floor; W-2 wall (middle wall) had very minor top sliding; diagonal crack extended below W-3 wall segment; max. 1st story drift = 0.21%; structural period T after test was about 0.10 s.
145% El Centro	Slightly below MCE	1.02 g	More flexural cracks developed at wall base of Wall W-1; a diagonal shear cracks developed in Wall W-1; horizontal crack extended at the top of W-2 wall (middle wall) segment, followed with shear sliding at that line; flexural-shear cracks developed below W-2 wall segment; distributed web-shear cracks formed in Wall W-3 in both directions; vertical cracks developed in the intersection between web and flange in in both 1st story T-walls; minor cracks observed in 2nd story wall segments in the edges of openings and control joints; horizontal flexural cracks develop near top and base of out of plane walls and flanges of in-plane walls; max. 1st story drift = 0.40%; structural period T after test was about 0.21 s.
160% El Centro	MCE	0.93 g	Structure was severely damaged; wide diagonal cracks formed in the 1st story W-2 and W-3 wall segments; the opened shear crack in wall segment W-2 extended through the flange; diagonals crushed; significant spalling of face shells adjacent to diagonal cracks; residual opening of the web-shear crack of 2.0 in.; wall W-2 (middle wall) slid on the top about 0.25 in.; opened flexural cracks at the base and top of out-of-plane walls in the 1st and 2nd stories; max. 1st storydrift = 1.90%, period T after test was 0.84 s.

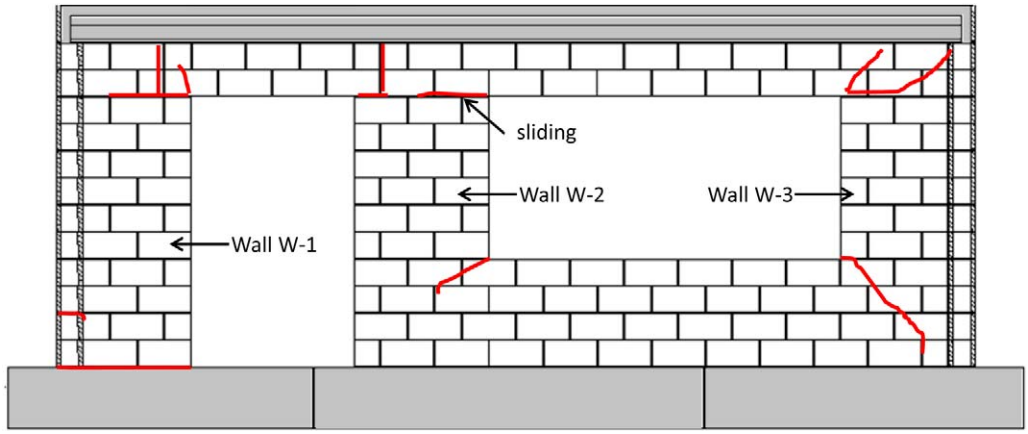

Figure 8. Observed cracks in first story of two-story specimen after 108% El Centro 1979 (DE).

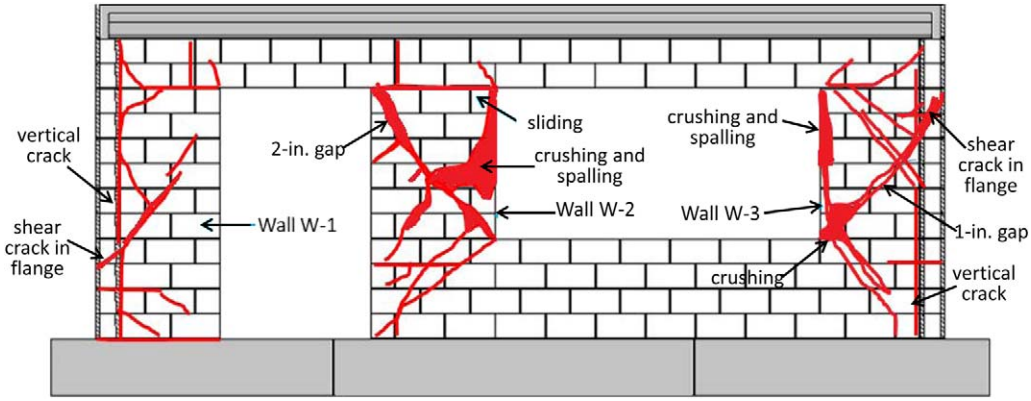

Figure 9. Observed damage in first story of two-story specimen after 160% El Centro (MCE).

produced vertical cracks along the length of Walls W-1 and W-3 (T-walls) between flanges and webs.

Because the diaphragms of the two-story specimen were essentially rigid in their own planes, overall behavior of the specimen was governed by the in-plane responses of Walls W-2 and W-3. Table 3 shows the results of the shake-table tests, including the maximum story drifts, base shears, and local deformation ratios in ground-level Walls W-1, W-2, and W-3. In this table, the shear deformation between the ends of each wall segment was calculated with the method recommended by Massone and Wallace (2004) using measurements from two diagonally oriented linear potentiometers in each wall segment. The shear deformation ratios are the calculated shear deformations divided by the height of the segment, and expressed in percent. Responses to ground motions before El Centro 30% are not shown in Table 3 because they were too small to be useful.

(a) (b) (c)

Figure 10. (a) Flexural and shear cracking in Wall W-1, (b) Wall W-2 after 160% El Centro, and (c) Wall W-3 after 160% El Centro.

COMPARISON BETWEEN SHAKE-TABLE TEST AND NUMERICAL RESULTS

In this section, the response of the two-story structure to the sequence of table motions was computed by nonlinear time history analysis, and the results were compared to the measured response of the structure. Results of the time-history analysis, summarized in Table 4, include the maximum predicted story drifts and local deformation demands in ground-level wall segments. In the interest of space, the numerical results are compared to the experimental results for the last 2 of the 6 input motions: 145% El Centro (between DE and MCE); and 160% El Centro (MCE).

For 145% El Centro, the predicted and measured first-floor displacement time-histories are shown in Figure 11. Response of the specimen was well captured. Peak displacements

Table 3. Overview of structural response of two-story specimen

Ground motion	Level of excitation	PGA (g)	Story drift in ground level, %		Base shear, kips	Maximum shear deformation ratio, %	
			West direction	East direction		Wall W-2	Wall W-3
30% El Centro	-	0.27	0.010	0.015	55	0.003	0.003
43% El Centro	0.50 DE	0.39	0.016	0.028	84	0.006	0.006
86% El Centro	0.80 DE	0.66	0.058	0.121	152	0.007	0.008
108% El Centro	DE	0.75	0.092	0.202	185	0.007	0.010
145% El Centro	below MCE	1.02	0.407	0.370	217	0.020	0.177
160% El Centro	MCE	0.92	1.825	1.062	221	2.470	1.524

Table 4. Results of time-history analysis for two-story specimen

Ground motion	Story drift in - ground level, %		Base shear, kips	Maximum local deformation, %		
	West direction	East direction		W-1	W-2	W-3
30% El Centro	0.05	0.07	73	0.09	0.13	0.12
43% El Centro	0.06	0.10	104	0.14	0.19	0.18
86% El Centro	0.10	0.23	158	0.28	0.44	0.44
108% El Centro	0.17	0.28	175	0.41	0.62	0.64
145% El Centro	0.28	0.42	195	0.59	0.95	0.98
160% El Centro	0.36	0.50	198	0.72	1.10	1.12

were predicted within 10%. The predicted and measured base shears are shown in Figure 12. As with displacements, response was well captured. Peak values are within 5% of the measured values. Hysteresis loops of base shear versus first-floor displacement are shown in Figure 13. Because the histories of first-floor displacements and base shears were accurately predicted, it is not surprising that the hysteresis loops also compare well. However, the analytical model shows slightly less nonlinearity than the experimental response.

An input motion of 160% El Centro measured from the table corresponds to shaking at MCE level, based on the fundamental period of the damaged structure right before the motion. For this motion, the predicted and measured first-floor displacement time-histories are shown in Figure 14. Due to the extensive damage to the specimen, its response was not well predicted. The predicted and measured base shears are shown in Figure 15. The base shear was well captured, even as the actual specimen was severely damaged with load degradation. Peak values are within 10% of the measured values. Hysteresis loops of base shear versus first-floor displacement are shown in Figure 16. Because the history of first-floor displacements was not accurately predicted, it is not surprising that the hysteresis loops

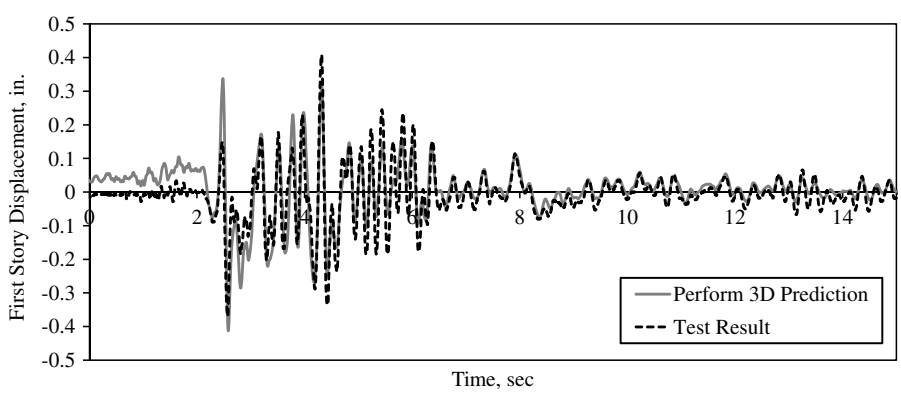

Figure 11. Time history of first-floor displacement for two-story specimen (145% El Centro).

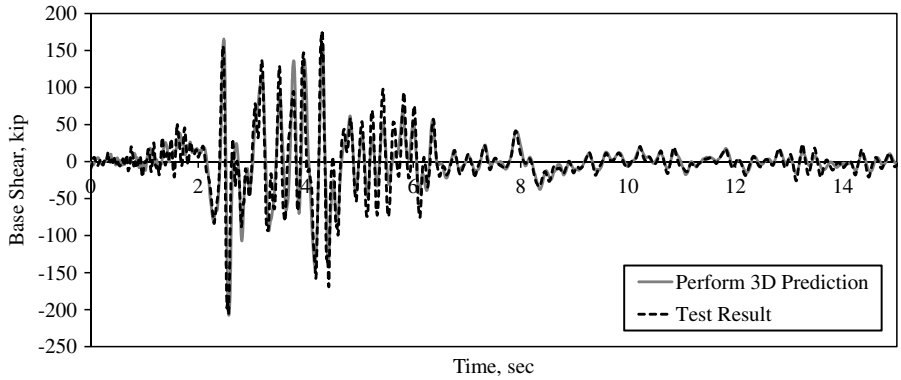

Figure 12. Time history of base shear for two-story specimen (145% El Centro).

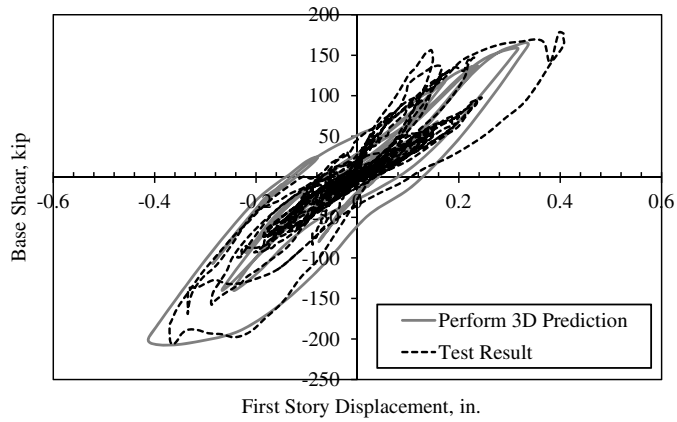

Figure 13. Load-displacement hysteresis loops for two-story specimen (145% El Centro).

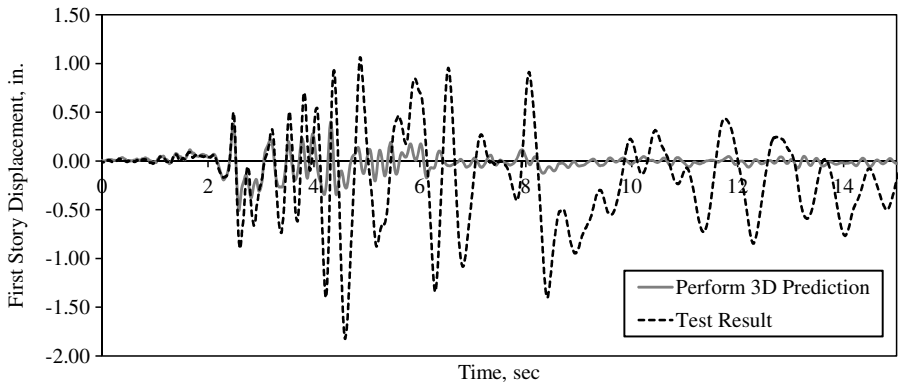

Figure 14. Time history of first-floor for two-story specimen (160% El Centro).

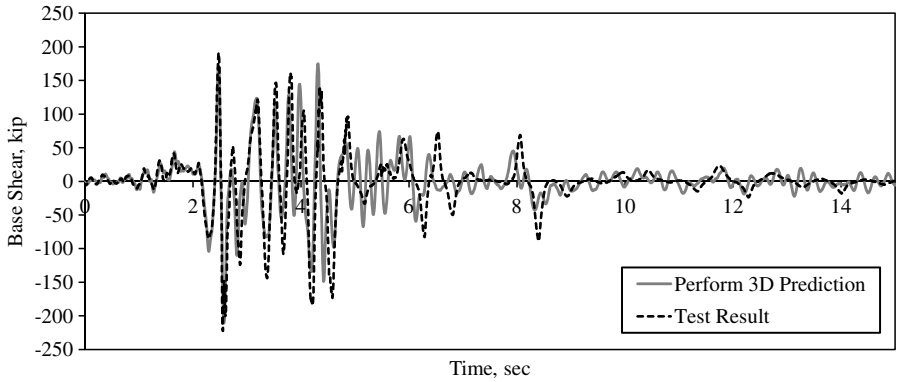

Figure 15. Time history of base shear for two-story specimen (160% El Centro).

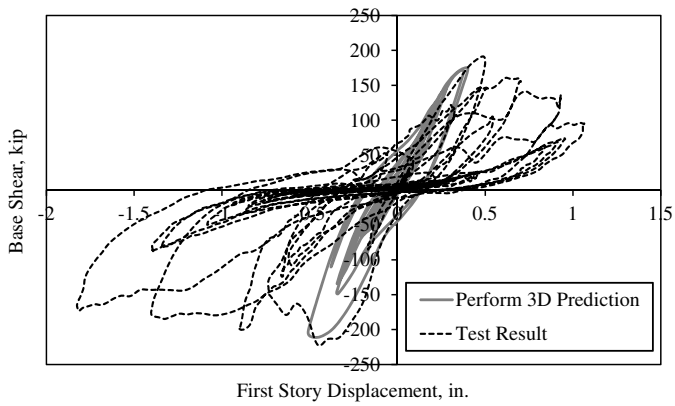

Figure 16. Load-displacement hysteresis loops for two-story specimen (160% El Centro).

also were quite different. In this shaking, the analytical model shows much less deformation, displacement, and nonlinearity than the experimental response. This was due to the inability of the "General Wall Elements" of PEFORM3D to simulate severe load degradation caused by diagonal shear failure and the sliding occurring at the top of Wall W-2.

Starting with the run using 145% El Centro, significant sliding was observed at the top of Wall W-2 during the tests. In an effort to improve the accuracy of analytical predictions, an attempt was made to model the possibility of extreme sliding by setting the capacity of shear layers in the top row of the General Wall Elements for Wall W-2 to the sliding shear capacity. However, the attempt was not successful. The modified model had almost the same deformation, displacement, and base shear as the original model. Hence, it is believed that the ability to simulate severe load degradation due to diagonal shear failure combined with sliding is of primary importance. Figure 17 shows the maximum predicted local deformation ratios in ground-level wall segments W-1, W-2, and W-3 and maximum story drift under

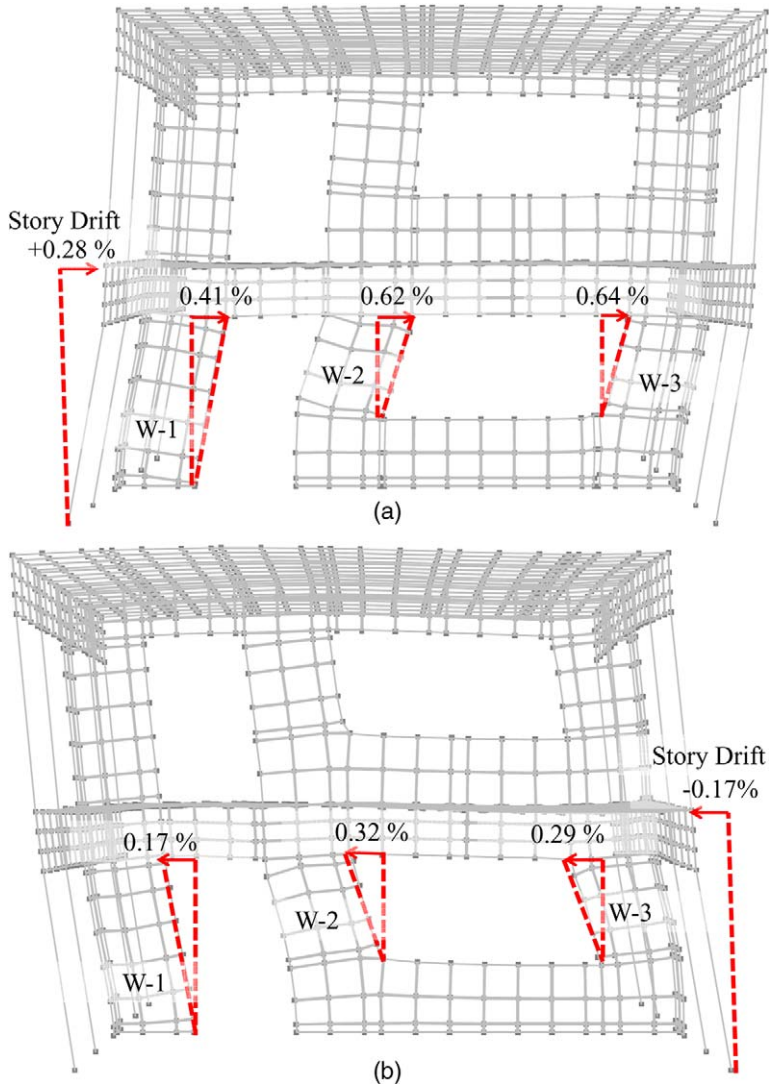

Figure 17. Maximum predicted local deformation ratios under 108% El Centro (DE level).

108% El Centro ground motion (DE). By comparing to the test result in Table 4, it can be seen that the story-drift at the ground level was well predicted. The local deformation demands for Walls W-2 and W-3 slightly exceeded the design limit of 0.5% for shear-controlled wall segments. Figure 18 shows local deformation ratios versus expected deformation capacities obtained with the analytical model for each ground-level wall segment over the test sequence. Walls W-2 and W-3 were critical, with the highest predicted local deformation ratios at the ground level, and the lowest deformation capacities, because these segments were shear-controlled. Comparing local drift-ratio demands with capacities for each ground-level wall segment, the two-story specimen can be expected to safely withstand 145%

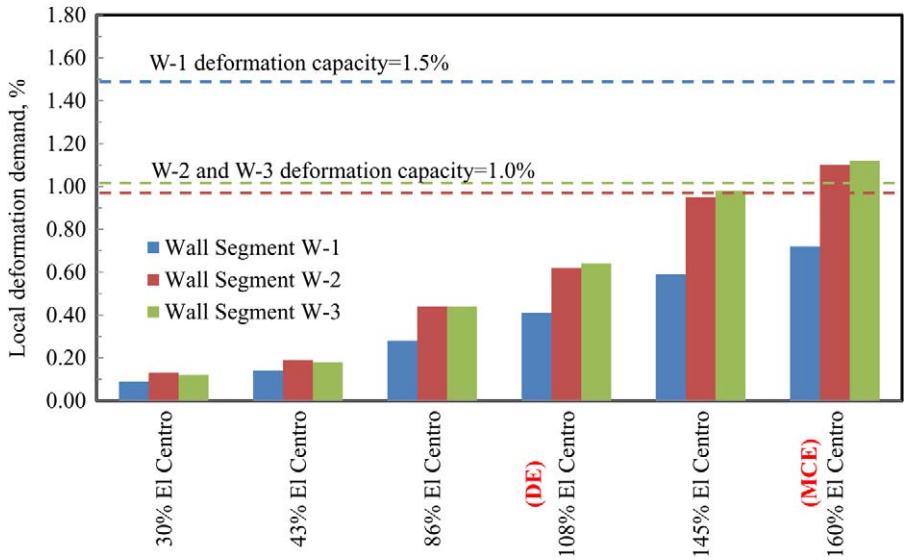

Figure 18. Deformation demand versus capacity for each ground-level wall segment over test sequence.

El Centro ground motion. However, under 160% El Centro ground motion (MCE), local deformation demands on wall segments W-2 and W-3 slightly exceed the expected deformation capacities. Based on the above comparison of experimental and numerical results, the local deformation demands for 160% El Centro were definitely significantly under-estimated in the numerical results.

The measured story drift in the ground floor is compared with the story drift limit used in the displacement-based design and the maximum story drift from the time history analysis for 160% El Centro ground motion (MCE). As shown in Figure 19, the story drift limit for MCE

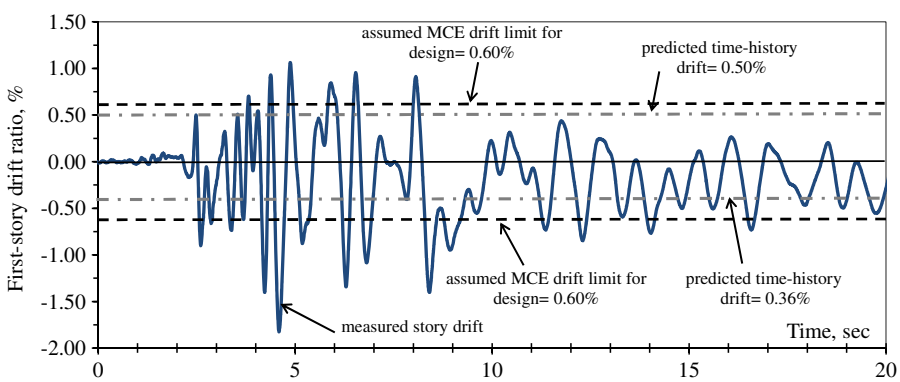

Figure 19. Comparison between measured and predicted story drift ratios for two-story specimen (160% El Centro).

used in the displacement-based design was 0.60%, corresponding to a local deformation demand in Wall W-2 of about twice that value. Under 160% El Centro, the measured story drift ratio (the blue curve) reaches maximum values of about +1.10% and −1.70%, considerably greater than the drifts predicted using time-history analysis, and also greater than the MCE drift limits used in the displacement-based design of the two-story specimen. Results show that the two-story specimen's local and global displacements were well predicted up to MCE, but not at MCE. At MCE, extensive shear degradation in shear-controlled wall segments caused the period of the specimen to increase to about 0.84 s. As shown in Figure 5, the response spectrum for 160% El Centro has two strong pulses between 0.21 s and 0.84 sec, indicating that the shaking was stronger than anticipated and exceeded the MCE level during the last run.

The total lateral deformation ratio of each wall segment is roughly the difference in displacement between the two ends of the segment divided by the distance between the two ends. It represents the summation of flexural, shearing, and sliding deformations. In the shake-table tests of the two-story specimen, differences in end displacements were not measured, so total lateral deformation ratios were not available. Shearing deformations in ground-level walls were measured, however, using data from two diagonally oriented and two vertically oriented potentiometers in each segment, and the calculation procedure of Massone and Wallace (2004). The measured shearing deformations (less than or equal to the total lateral deformations) in Walls W-2 and W-3 at ground level was used to estimate the total lateral deformations of those walls, which can then be compared with the expected total lateral deformation capacities of those wall segments based on quasi-static tests.

Based on the results from quasi-static tests of fixed-fixed specimens with an aspect ratio of 1.0 and low axial load ratios (similar to that of Wall W-2 and Wall W-3), the average ratio of displacement from shearing deformations to total displacement (excluding sliding-shear deformations) at the end of the tests was 0.64 (Ahmadi 2012). Therefore, dividing the measured shearing deformation ratios in Walls W-2 and W-3 by 0.64 gives an estimate of the total deformation ratios (flexural plus shearing deformations) of those wall segments. These estimated total deformation ratios then were compared with the expected total deformation capacities for shear-controlled wall segments.

In Figures 20 and 21, estimated total deformation ratios are compared with expected total deformation capacities for ground-level Walls W-2 and W-3. For Wall W-2 (Figure 20), total deformation ratios estimated using measured shearing deformation ratios reached almost 1.80% in the positive direction and almost 3.80% in the negative direction, much greater than the expected total deformation capacity ratio of 1.00% at the MCE level. For Wall W-3 (Figure 21), total deformation ratios estimated using measured shearing deformation ratios reached almost 1.90% in the positive direction and almost 2.40% in the negative direction, considerably greater than the expected total deformation capacity ratio of 1. Based on the successful performance of the specimen without collapsing at these local deformation ratios, the proposed total lateral deformation limits of 1.00% for shear-dominated walls with closely spaced orthogonal reinforcement seems reasonable and perhaps even conservative. The results also show that under dynamic loading, the wall segments reached and even surpassed the lateral deformation limits based on cyclic load tests.

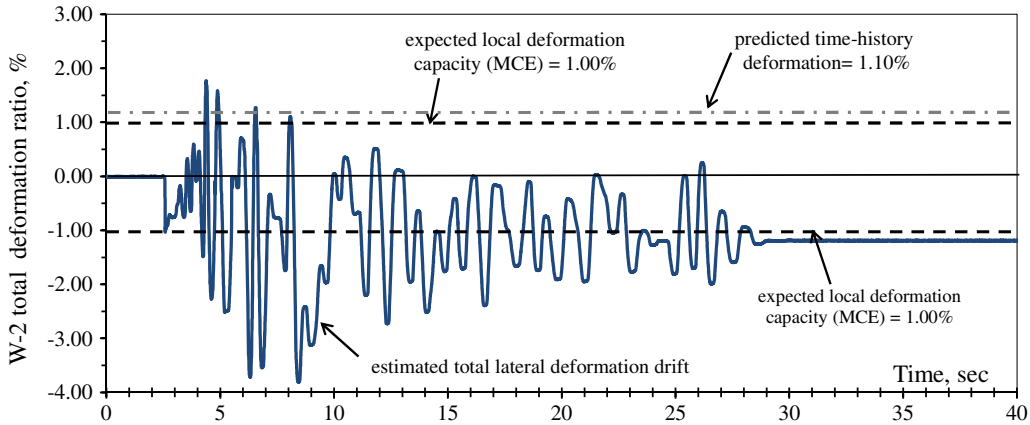

Figure 20. Comparison between estimated total lateral deformation ratios and expected total deformation capacity for Wall W-2 (160% El Centro).

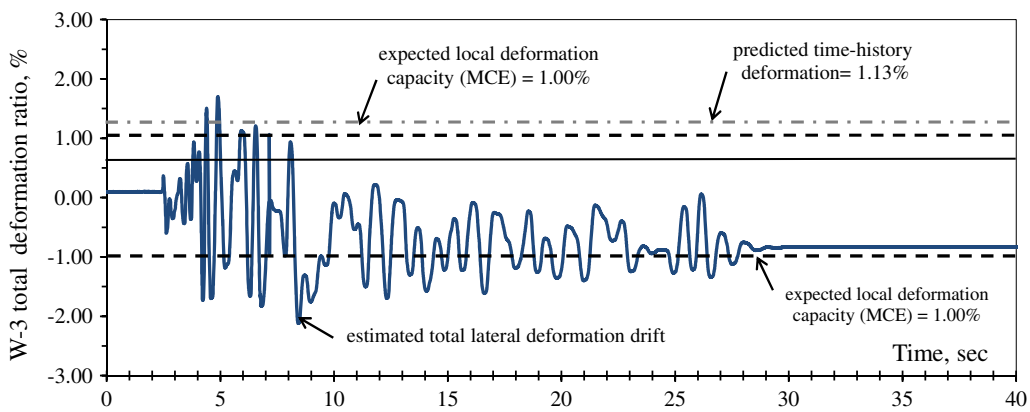

Figure 21. Comparison between estimated total lateral deformation ratios and expected total local deformation capacity for Wall W-3 (160% El Centro).

As a final remark, it is important to point out that the test specimen was subjected to a sequence of demanding ground motions, that is, 108%, 145%, and 160% El Centro, with significant period elongation after 145% El Centro. Pre-test analyses presented here have shown that the maximum story drifts and local deformation demands would be a lot less if the undamaged structure were subjected to MCE level motions, only slightly violating the proposed design limits. Code provisions (ASCE 2010) for seismic design are intended to have a low probability of collapse (no more than 10%) under MCE. The fact that the test specimen experienced repeated strong shakings up to the MCE level without collapsing is strong evidence that the design is satisfactory.

CONCLUSIONS

The research described here provides a comprehensive validation of a displacement-based seismic design procedure for reinforced masonry structures. A full-scale, two-story specimen was tested on a shake table to examine the global and local behaviors of a low-rise reinforced masonry building designed by the proposed displacement-based procedure and to validate the analytical tool used in the design process. This specimen resisted repeated ground motions with intensities up to the Maximum Considered Earthquake (MCE). The specimen experienced extensive damage when subjected to ground motions with intensities exceeding MCE level, and severe diagonal cracks developed in shear-dominated wall segments. In critical regions of this specimen, elements detailed in accordance with displacement-based design requirements showed more inelastic deformation capacity than the deformation limits imposed by the displacement-based design provisions proposed in this paper. The procedure produces structures that behave reliably in strong earthquakes. It is more consistent and transparent than current force-based seismic design procedures. It can be used for structures with configurations of openings that are difficult or practically impossible for force-based design, and that are commonly encountered in practice. It is suitable for use by experienced design offices.

Provisions permitting displacement-based seismic design procedures should be incorporated into ASCE 7. Corresponding provisions permitting displacement-based design should be included in future editions of the MSJC *Code* (2011).

ACKNOWLEDGMENTS

The material reported in this paper is based upon a multi-university research project supported by the United States National Institute of Standards and Technology (NIST ARRA Measurement Science and Engineering Grant award No. 60NANB10D013). That project used shaking-table facilities at the University of California at San Diego, provided by the United States National Science Foundation's Network for Earthquake Engineering Simulation (NSF NEES).

REFERENCES

Abrams, D., and Paulson, T., 1991. Modeling earthquake response of concrete masonry building structures, *ACI Struct. J.* **88**, 475–485.

Ahmadi, F., Mavros, M., Klingner, R. E., Shing, B., and McLean, D., 2015. Displacement-based seismic design for reinforced masonry shear-wall structures, part 1: Background and trial application, *Earthquake Spectra* **31**, 969–998.

American Society of Civil Engineers (ASCE), 2010. *ASCE/SEI 7-10: Minimum Design Loads for Buildings and Other Structures* (ASCE 7-10), American Society of Civil Engineers, Reston, VA.

American Society for Testing and Materials, 2012. *ASTM C270-12: Standard Specification for Mortar for Unit Masonry*, American Society for Testing and Materials, West Conshohocken, PA.

American Society for Testing and Materials, 2010. *ASTM A476-10: Standard Specification for Grout for Masonry*, American Society for Testing and Materials, West Conshohocken, PA.

American Society for Testing and Materials, 2011. *ASTM C90-11a: Standard Specification for Loadbearing Concrete Masonry Units*, American Society for Testing and Materials, West Conshohocken, PA.

Ahmadi, F., 2012. Displacement-based Seismic Design and Tools for Reinforced Masonry Shearwall Structures, Ph.D. Thesis, The University of Texas at Austin.

Cohen, G. L., Klingner, R. E., Hayes, J. R., Jr., and Sweeney, S., 2004a. Seismic response of low-rise masonry buildings with flexible roof diaphragms, part I: Seismic and quasi-static testing, *Earthquake Spectra* **20**, 779–801.

Cohen, G. L., Klingner, R. E., Hayes, J. R., Jr., and Sweeney, S., 2004b. Seismic response of low-rise masonry buildings with flexible roof diaphragms, part II: Analytical modeling, *Earthquake Spectra* **20**, 803–824.

Computers & Structures, Inc. (CSI), 2007. *PERFORM-3D V5, Nonlinear Analysis and Performance Assessment for 3D Structures*, Berkeley, California.

Gülkan, P., Clough, R. W., Mayes, R. L., and Manos, G., 1990a. Seismic testing of single-story masonry houses, Part I, *J. Struct. Eng.* **116**, 235–256.

Gülkan, P., Clough, R. W., Mayes, R. L., and Manos, G., 1990b. Seismic testing of single-story masonry houses, Part II, *J. Struct. Eng.* **116**, 257–274.

Jo, S., 2010. Seismic Behavior and Design of Low-rise Reinforced Concrete Masonry with Clay Masonry Veneer, Ph.D. Thesis, The University of Texas at Austin.

Klingner, R. E., Shing, B., McGinley, W. M., McLean, D. I., Okail, H., and Jo, S., 2010. Seismic performance tests of masonry and masonry veneer, *Journal of ASTM International* **7**.

Harris, H. G., and Sabnis, G. M., 1999. *Structural Modeling and Experimental Techniques*, CRC Press, Boca Raton, FL, 808 pp.

Massone, L. M., and Wallace, J. W., 2004. Load-deformation responses of slender reinforced concrete walls, *ACI Structural Journal* **101**, 103–113.

Masonry Standards Joint Committee (MSJC), 2011. *Building Code Requirements for Masonry Structures* (TMS 402-11/ACI 530-11/ASCE 5-11), The Masonry Society, Boulder, CO; the American Concrete Institute, Farmington Hills, MI; and the American Society of Civil Engineers, Reston, VA.

Ozcelik, O., Luco, J. E., Conte, J. P., Trombetti, T. L., and Restrepo, J. I., 2008. Experimental characterization, modeling and identification of the NEES-UCSD shake table mechanical system, *Earthquake Eng. Struct. Dyn.* **37**, 243–264.

Seible, F., Hegemier, A., Igarashi, A., and Kingsley, G., 1994a. Simulated seismic-load tests on full-scale five-story masonry building, *J. Struct. Eng.* **120**, 903–924.

Seible, F., Priestley, N., Kingsley, G., and Kurkchubashe, A., 1994b. Seismic response of full-scale five-story reinforced-masonry building, *J. Struct. Eng.* **120**, 925–947.

Stavridis, A., Koutromanos, I., and Shing, P. B., 2012a. Shake-table tests of a three-story reinforced concrete frame with masonry infill walls, *Earthquake Engng Struct. Dyn.* **41**, 1089–1108.

Stavridis, A., Ahmadi, F., Mavros, M., Shing, P., Klingner, R. E., and McLean, D., 2012b. Shake-table testing of a 3-story, full-scale reinforced masonry wall system, in *The 15th International Brick and Block Masonry Conference*, Florianopolis, Brazil.

(Received 2 December 2012; accepted 5 July 2013)